Fabrication and modal characterisation of large-area polymer membranes for acoustic micro-electromechanical systems devices

Luca Camellini[1,2], Alberto Torin[3], Asaad K. Al-mashaal[1], Graham S. Wood[1], Michael J. Newton[3], Rebecca Cheung[1], Enrico Mastropaolo[1] ✉

[1]*School of Engineering, Institute for Integrated Micro and Nano Systems, The University of Edinburgh, Edinburgh, UK*
[2]*Politecnico di Torino, Torino (TO), Italy*
[3]*Acoustics and Audio Group, Edinburgh College of Art, The University of Edinburgh, Edinburgh, UK*
✉ *E-mail: e.mastropaolo@ed.ac.uk*

Published in Micro & Nano Letters; Received on 2nd February 2018; Revised on 20th March 2018; Accepted on 27th March 2018

Bilayer polymer/metal suspended membranes made of poly(methyl methacrylate) (PMMA) and aluminium (Al) have been fabricated using a wet transfer technique where a polyelectrolyte (polydiallyldimethylammonium chloride – PDAC) has been employed as sacrificial layer to facilitate the detachment of the thin PMMA/Al layers from the substrate holders. In this way, free-standing PMMA/Al membranes with outstanding diameter (3.5 mm) to thickness (400 nm) ratios of $\sim 10^4$ have been obtained. The membranes have been actuated mechanically and electrothermally and their modal behaviour characterised using laser Doppler vibrometry. The first five modes of vibrations have been detected in the range of 2–25 kHz. The second and fifth degenerate modes have been seen to split, probably due to non-uniform tension or mass density. The membranes can achieve vibration amplitudes in the order of few tens of microns. When performing electro-thermal actuation, it has been observed that the amplitude of a single mode can be tuned by controlling the path of the electric current across the membrane.

1. Introduction: Free-standing micro-electromechanical systems (MEMS) membranes with large diameter to thickness ratios are attracting broad attention for acoustic applications. Single/multi-layer graphene, polymers or graphene/polymer membranes [1] have been used for developing MEMS microphones [2], loudspeakers [3], ultrasonic transducers [4], and highly flexible capacitive sensors [5]. Large surface areas, combined with the possibility of using polymers as structural materials, allow the membranes to resonate in the audio range (20 Hz–20 kHz). This makes them particularly suitable for biomimetic microphones or sound absorption devices [6]. In addition, polymer MEMS are becoming more ubiquitous, targeting a wide range of applications for sensors and actuators [7] offering cost-effective novel and improved functionalities [8, 9].

The fabrication of large-area (and high diameter/thickness ratio) MEMS polymer-based membranes presents several challenges when utilising standard micromachining techniques (i.e. lithography, and surface or bulk dry micromachining). In particular, many polymers have limited compatibility with photoresists and etching processes. Removal of sacrificial layers or bulk materials, without damaging the large and thin membrane structure, makes fabrication extremely challenging. However, wet transfer techniques overcome the need for etching sacrificial layers or substrates, and are therefore appropriate for ultra-thin materials which cannot be grown or deposited on standard substrates used for silicon technology.

Wet transfer techniques have proven rather successful for the fabrication of free-standing graphene membranes, with a relatively high yield [10]. Large aspect ratio free-standing membranes can be fabricated by using water-soluble polymers, such as polyelectrolytes. These polymers can be used as sacrificial layers [11], or for building multilayers structures [12]. In addition, water-soluble polymers can facilitate delamination by modifying the surface of silicon substrates [13], reducing the roughness of the film. However, whilst surface modification is suitable for polymeric membranes, it falls short when metal electrode layers are needed on the polymer membrane.

In this Letter, we present a novel approach for the fabrication of high diameter to thickness ratio ($\sim 10^4$) bilayer polymer/metal membranes. A polyelectrolyte (polydiallyldimethylammonium chloride – PDAC) was used as a sacrificial layer to facilitate detachment of the polymer/metal (PMMA/aluminium, Al) film from a silicon substrate [13]. The detached film was further transferred over a silicon cavity, thus forming a free-standing polymer/metal membrane. The fabricated membranes were actuated mechanically and electrothermally, and their modal behaviour characterised.

2. Experimental procedure: The fabrication process involved preparation of the membranes and cavities on two separate substrates. The membranes were subsequently transferred onto the cavities using a wet transfer procedure. Fig. 1 shows the schematic process flow for the fabrication of the devices.

To fabricate the cavities, an insulating layer of silicon dioxide (SiO_2) (275 nm) was deposited on a silicon (Si) substrate (380 μm thick) by chemical vapour deposition. Afterwards, to provide an electrical connection to the chip containing the cavities, a 300 nm thick Al layer was sputtered on top and electrode pads patterned using a lift-off process. Circular cavities (diameter of 3.5 mm) were first created by reactive ion etching (RIE) of the SiO_2, and subsequently by deep reactive ion etching (DRIE) to create a hole through the Si wafer. The wafer was then diced into 7×7 mm^2 chips, each containing a single cavity.

The polymer/metal membranes were fabricated using Si substrates as holders. Initially, the Si substrates were cleaned in a piranha solution (H_2SO_4:H_2O_2(30 wt%) = 3:1), rinsed in deionised water and dried. Afterwards, the substrates were coated with PDAC (Sigma-Aldrich, average M_w 100,000–200,000) 5 wt% spun at 4000 rpm for 15 s, then baked at 100°C for 1 min. After creation of the PDAC sacrificial layer, an 80 nm thick Al layer was sputtered, followed by spinning of PMMA (Sigma-Aldrich, average M_w 960,000) 5 wt% in anisole at 1000 rpm for 30 s. The resulting substrates were then baked at 60°C for 5 min, resulting in a 340 nm thick PMMA layer on top of the Al. The PMMA/Al

doi: 10.1049/mnl.2018.0089

layer was incised using a razor blade to define the membranes ($\sim 5\times 5$ mm^2) and facilitate detachment from the Si substrates.

The PMMA/Al layers were isolated by immersing the Si substrate holders in deionised water. In this way, the PDAC sacrificial layer was dissolved and the released PMMA/Al membranes were left floating on the water surface. Successively, the floating membranes were captured and transferred onto the cavity-bearing chips, and dried at room temperature for 30 min.

Devices incorporating suspended PMMA/Al membranes can be actuated mechanically or electrothermally. For mechanical testing, the devices were attached to a piezoelectric disk (15 mm diameter, 6 kHz resonant frequency) using carbon adhesive tape. The piezoelectric disk was then actuated with an 8 V AC voltage. For electrothermal testing, the devices were actuated by positioning two micromanipulators on the patterned Al electrode pads (1–8 in Figs. 2*a* and 2*b*) and applying 2 V AC voltage superimposed upon a 2 V DC voltage [1, 14]. The frequency response of the membranes was investigated in the range of 1–35 kHz using a laser Doppler vibrometer (LDV) (Polytec MSA-050). Velocity measurements were performed using a periodic chirp as the input signal, with the resulting out-of-plane membrane velocity recorded at multiple points across its surface. This allowed the full 2D deflection profile (as a function of frequency) to be reconstructed, permitting identification of modal patterns. A number of points outside the membrane were measured as a reference, to enable subtraction of any background vibration of the substrate.

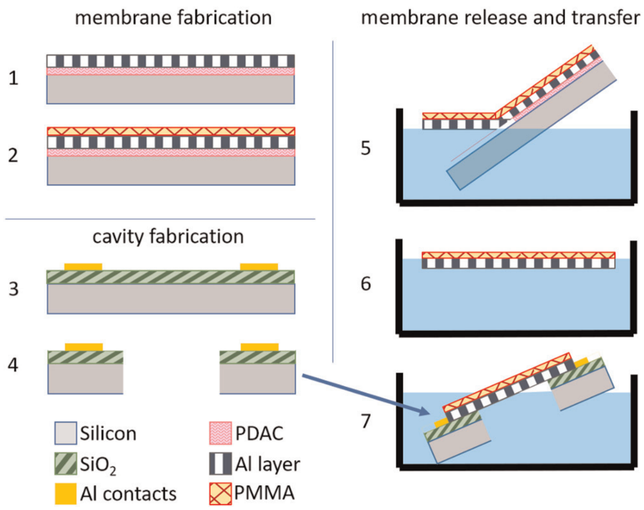

Fig. 1 *Process flow schematic. Membrane: (1) an Al layer is sputtered on a sacrificial PDAC layer spin coated on a Si substrate; (2) PMMA is spin coated. Cavities: (3) SiO_2 is deposited on a Si substrate, Al electrodes are patterned with lift-off; (4) the cavity is created by RIE and DRIE. Transfer: (5) substrate with membrane is immersed in DI water, (6) resulting in the release of the membrane; (7) membrane is transferred onto the cavity and dried at room temperature*

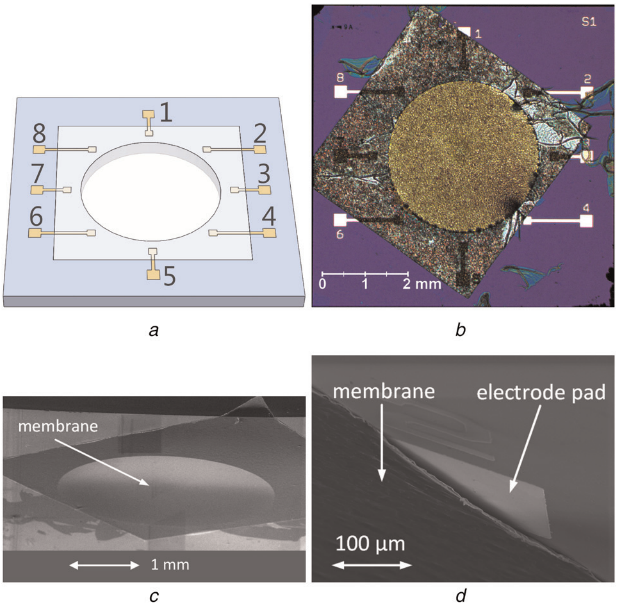

Fig. 2 *Large-area PMMA/Al membranes with Al contact pads for electrical actuation*
a Device schematic; and final device:
b Optical image, scanning electron micrograph of
c Entire membrane and
d Membrane detail with electrode pad

3. Results and discussion: Fig. 2 shows the schematic of the designed devices together with an optical image and scanning electron micrograph of one of the fabricated devices. The suspended membranes have a diameter of 3.5 mm, and a total thickness of ~400 nm, resulting in an aspect ratio of $\sim 10^4$.

Membrane surfaces tended to develop a series of small ridges, evident in Fig. 2. This was likely due to slight shrinkage of the membrane whilst it floated on the deionised water, releasing some of the residual stress acquired during the fabrication process. It was noticed that the size of the ridges was affected by the fabrication process parameters, in particular by the temperature at which the PMMA solvent was evaporated (i.e. the heating step performed after spin-coating the PMMA).

Fig. 3 shows the average spectrum, after background subtraction, obtained from each of the mechanical and electrothermal actuation processes. In the second case, in order to maximise the current flowing through the centre of the membrane and thus maximise the amplitude of the first mode [1], the device was actuated using opposite pads (i.e. electrodes 2 and 6 in Fig. 2). As shown in Fig. 4, the first five vibration modes, corresponding to the various peaks in Fig. 3, were clearly observable. Table 1 summarises the observed resonant frequencies of a device tested using both mechanical and electrothermal actuation, and demonstrates that that the first four modes were in the human hearing range (mode 1 = 2.53 kHz, mode 2 = 9.65–10.1 kHz, mode 3 = 16 kHz, mode 4 = 16.9 kHz). In an ideal circular membrane, all the non-axisymmetric modes (those without circular symmetry) are degenerate, meaning that two modes, identical but for a rotation, share the same frequency. In the present device, however, two peaks were

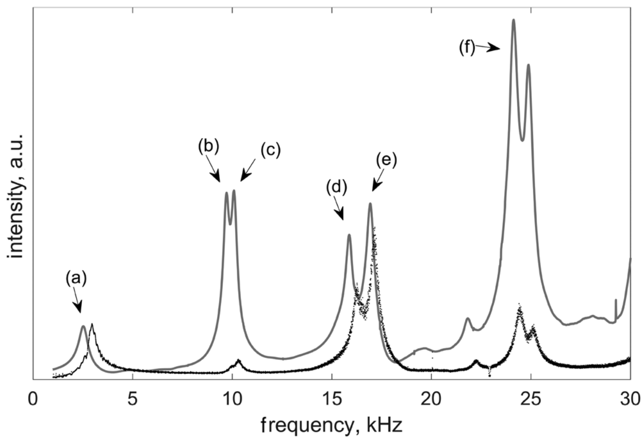

Fig. 3 *Velocity spectrum with mechanical (solid grey line) and electrothermal (dotted black line; actuation pads 2 and 6) actuation, normalised to the intensity of the first resonant peak. The letters on the peaks correspond to the resonant modes shown in Fig. 4*

doi: 10.1049/mnl.2018.0089

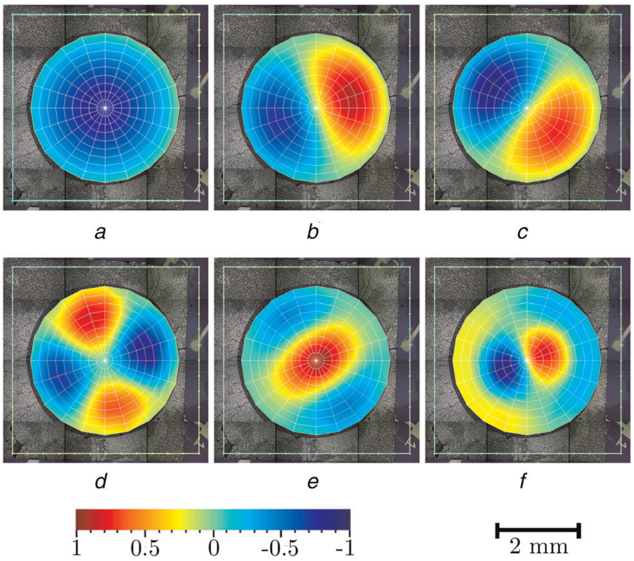

Fig. 4 *Vibration modes measured with LDV. The intensity of vibration is normalised*
a Fundamental mode
b, *c* Second mode, non-degenerate
d Third
e Fourth
f Fifth

Table 1 Frequencies of the first five resonant modes, for both mechanical and electrothermal actuation. Note the frequency splitting of the second and fifth mode

Mode	Frequency, kHz	
	Mechanical act.	Electrothermal act.
1	2.53	2.96
2	9.65	10.0
	10.1	10.3
3	16.0	16.3
4	16.9	17.2
5	24.1	24.4
	24.9	25.2

observed for the second and fifth mode. The degeneracy in this case was broken (see Figs. 3*b* and *c*), and two modes with slightly different frequencies, 9.65 and 10.1 kHz for mechanical actuation, were observed. Furthermore, the large deflections when actuating mechanically and the Joule heat induced when actuating electrothermally influence the membrane's effective stiffness. As a result, the mode frequency values detected with electrothermal actuation are higher than the ones detected with mechanical actuation (see Table 1).

In the case of mechanical actuation, the membrane's vibration intensity was strictly related to the amplitude of vibration of the piezo disk; this can vary greatly depending on the quality of the mounting to the substrate. The measurements showed the membrane to be vibrating at 200 mm/s (first mode), corresponding to a displacement of∼13 μm, 20 times higher than the displacement of the piezo disk. The displacement obtained with electrothermal actuation of the membrane was three orders of magnitude lower but increased with higher actuation voltages. The devices characterised here were actuated using a short periodic chirp thus showing the same resonant behaviour consistently over multiple tests. However, over sustained periods of actuation, which will be necessary in practical audio applications, it is likely that the mechanical properties of the membrane, such as the effective stiffness, will alter, resulting in a shift in the resonant behaviour.

In the case of electrothermal actuation, the amplitude of the second mode was almost negligible, most likely due to the presence of a current flowing through the centre of the membrane, where the modal displacement should be close to zero. This assumption is supported by the fact that when using adjacent pads (e.g. pads 2–4) for the actuation, the amplitude of the first mode was reduced while the second mode was increased compared to the case of actuation with opposite pads (e.g. pads 2–6); in this case, the current flowing through the centre of the membrane was lower and a higher current flowed through the side of membrane, which induces Joule heating that more efficiently actuates non-axisymmetric modes. The overall intensity of oscillation was non-linearly proportional to the AC actuation voltage applied to the electrodes, which is a result of the increased AC current flowing through the membrane, inducing increased Joule heating.

4. Conclusions: Large surface area polymer/metal (PMMA/Al) membranes with diameter (3.5 mm) to thickness (400 nm) ratios of $\sim 10^4$ were fabricated by wet transfer in combination with a polyelectrolyte (PDAC) sacrificial layer. An Al metal layer allowed for electrical connection to the structure. The membranes were actuated mechanically and electrothermally, allowing observation of the first five vibration modes with resonant frequencies in the range of 2–25 kHz (with the first four modes being in the human hearing range). Despite the relatively large amplitudes detected with mechanical actuation (∼13 μm), the devices did not show any major reliability issue over multiple testing. Vibration amplitudes up to 20 nm were measured when actuating the membranes electrothermally using a 2 V AC voltage superimposed upon 2 V DC. The amplitude could be increased by increasing the actuation voltage. In addition, the relative amplitude of the mode shapes could be tuned by forcing the electric current to follow specific paths across the membrane. Mode splitting of the degenerate mode shapes was observed, most likely due to non-uniform surface properties of the membrane (non-uniform tension or mass density), which breaks the symmetry of the non-axisymmetric modes causing a splitting of their frequencies. The obtained mode shapes matched well with those expected by analytic consideration of circular membranes.

This Letter demonstrates the manufacturing of millimetric membranes that resonate in the human hearing range, and which may be used to design innovative biomimetic acoustic devices such as microphones and sound absorbers. Furthermore, the described fabrication process allows for facile integration of large-area membranes on hybrid microsystems.

5 References

[1] Al-mashaal A.K., Wood G.S., Torin A.: 'Dynamic behavior of ultra large graphene-based membranes using electrothermal transduction', *Appl. Phys. Lett.*, 2017, **111**, 243503, pp. 1–4

[2] Todorovic D., Matkovic A., Milicevic M.: 'Multilayer graphene condenser microphone', *2D Mater.*, 2015, **2**, 045013, pp. 1–6

[3] Zhou Q., Zettl A.: 'Electrostatic graphene loudspeaker', *Appl. Phys. Lett.*, 2013, **102**, 223109, pp. 1–5

[4] Chong P.-F., Cheng C.-H., Shi X.: 'Capacitive micromachined ultrasonic transducer (CMUT) array with single-layer graphene membrane', *Micro & Nano Lett.*, 2014, **9**, (12), pp. 884–886

[5] Ahmad Ridzuan N.A., Miki N., Masuda S.: 'Flexible capacitive sensor encapsulating liquids as dielectric with a largely deformable polymer membrane', *Micro & Nano Lett.*, 2012, **7**, (12), pp. 1193–1196

[6] Yanga Z., Dai H.M., Chan N.H.: 'Acoustic metamaterial panels for sound attenuation in the 50–1000 Hz regime', *Appl. Phys. Lett.*, 2010, **96**, 041906, pp. 1–3

[7] Kim B.J., Meng E.: 'Review of polymer MEMS micromachining', *J. Micromech. Microeng.*, 2016, **26**, 013001, pp. 1–22

doi: 10.1049/mnl.2018.0089

[8] Kottapalli A.G.P., Tan C.W., Olfatnia M.: ‘A liquid crystal polymer membrane MEMS sensor for flow rate and flow direction sensing applications’, *J. Micromech. Microeng.*, 2011, **21**, 085006, pp. 1–11
[9] Dusek J., Kottapalli A.G.P., Woo M.E.: ‘Development and testing of bio-inspired microelectromechanical pressure sensor arrays for increased situational awareness for marine vehicles’, *Smart Mater. Struct.*, 2013, **22**, 014002, pp. 1–13
[10] Suk J.W., Kitt A., Magnuson C.W.: ‘Transfer of CVD-grown monolayer graphene onto arbitrary substrates’, *ACS Nano*, 2011, **5**, pp. 6916–6924
[11] Linder V., Gates B.D., Ryan D.: ‘Water-soluble sacrificial layers for surface micromachining’, *Small*, 2005, **1**, (7), pp. 730–736
[12] Dubas S.T., Farhat T.R., Schlenoff J.B.: ‘Multiple membranes from ‘true’ polyelectrolyte multilayers’, *J. Am. Chem. Soc.*, 2001, **123**, (22), pp. 5368–5369
[13] Baxamusa S.H., Stadermann M., Aracne-Ruddle C.: ‘Enhanced delamination of ultrathin free-standing polymer films via self-limiting surface modification’, *Langmuir*, 2014, **30**, (18), pp. 5126–5132
[14] Mastropaolo E., Cheung R.: ‘Electrothermal actuation studies on silicon carbide resonators’, *J. Vac. Sci. Technol. B Microelectron. Nanom. Struct.*, 2008, **26**, (6), pp. 2619–2623

doi: 10.1049/mnl.2018.0089